

APPLE UNDULATORS FOR HGHG-FELS

J. Bahrtdt, BESSY, Berlin, Germany.

Abstract

Cascaded HGHG-FEL facilities have been proposed by several groups. In these machines the beam characteristics of the initial seeding laser like coherence, short time structure and small bandwidth are transformed to shorter wavelengths where seeding lasers are not available. The first stages are equipped with planar devices. For full polarization control the last amplifier and the final radiator can be realized as APPLE devices. The specific demands on the polarizing devices as compared to planar hybrid devices are discussed for the example of the proposed BESSY HE-FEL to be operated at 1nm. The field optimization procedure requires specific strategies. An improvement of the magnetic material is helpful in this context. The small good field region implies tight geometrical tolerances. Gap and phase dependent focussing effects have to be compensated. Other important issues are the complexity of the control system and the radiation protection system.

INTRODUCTION

FEL facilities are powerful sources for ultra short pulses and longitudinally and transversely coherent radiation in the soft X-ray and X-ray regime. Three X-ray FELs based on the SASE principle are currently under construction [1-3].

In the soft X-ray regime various seeding schemes have been proposed and realized which improve the spectral characteristics and the time structure. A cascaded HGHG FEL [4,5] starts with the coherent radiation of a high power Ti:Sapphire laser which interacts with the electron beam in a modulator. In a dispersive section the energy modulation is converted to a spatial modulation. The following radiator takes advantage of the higher orders of the electron beam bunching producing a seed for the next stage. Several stages can be cascaded achieving frequencies down to 1nm.

The number of stages can be reduced if the seed wavelength of the first stage is already in the few 10s nm regime which can be accomplished using the HHG process [6].

Only the light of the last radiator will be delivered to the experiment. All other undulator modules serve to provide a sufficient bunching of the electron beam in the last stage. For simplification all these modules can be realized as planar devices though they might be slightly longer than helical devices. The last radiator has to provide the full flexibility concerning the polarization control. APPLE type structures are suitable for this purpose. In this paper we concentrate on the design of APPLE undulators to be used as final radiators. We discuss the technical challenges and their solutions. For

illustration we will apply the parameters of the proposed BESSY Soft X-Ray FEL.

The tolerances for HGHG and SASE FEL undulators are similar for comparable photon energies. The complexity of a HGHG undulator system is, however, higher. A 200m SASE undulator consists of 40 identical 5m modules whereas a cascaded FEL can be composed of 18 modules with 9 different lengths and 5 different period lengths (BESSY HE-FEL). This affects the concept of series production and modularity, the control system and the operation.

In contrast to an X-ray FEL undulator system the undulator focussing is an important issue for soft X-ray systems (in particular for polarizing devices) because the electron energies are generally lower.

MAGNETIC STRUCTURE

APPLE undulators provide the highest fields among all variably polarizing insertion devices. A single pass FEL permits the installation of a circular beam pipe without performance loss. In this geometry additional magnetic material can be arranged at the side of the vacuum chamber. Additionally, the angle of magnetization can be rotated by 45° (APPLE III [7]). The demagnetizing fields are slightly higher for an APPLE III than for an APPLE II (figure 1). The magnetic stability can be recovered with another magnet grade and the field gain is still about a factor of 1.4 as compared to an APPLE II [7].

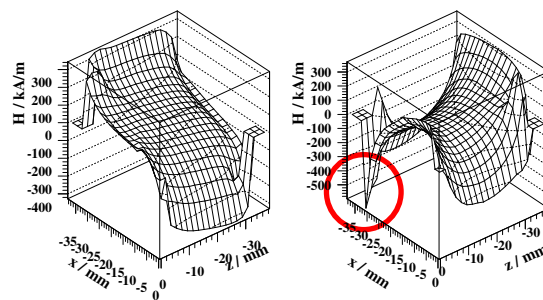


Figure 1: Difference of reverse fields between APPLE III and APPLE II design for the example of the planned BESSY UE50 (LE- and ME-FEL). Left: A-magnet (long. magnetized), right: B-magnet (vert. magnetized).

Today APPLE undulators can be built with the same field quality as planar devices using specific sorting and shimming techniques. At BESSY the magnets of the APPLE undulators are characterized individually with respect to the dipole moment (automated Helmholtz coil) and the inhomogeneities (stretched wire system). The data are used in a simulated annealing code which

minimizes the phase errors and reduces the multipoles by a factor of 5-10 as compared to an unsorted structure [8]. The field quality of devices consisting of 1000 magnets can be predicted with an accuracy of about 1.5 Gm (figure 2).

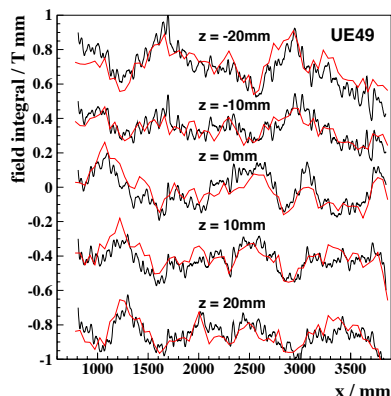


Figure 2: Prediction from single block characterization (red) and Hall probe measurements (black) of the BESSY UE49 field integrals at five transverse positions.

The field properties are optimized with various techniques:

- trajectories: block movements
- shift dependent terms: Fe-shims
- shift independent terms: permanent magnet arrays at both ends of the devices.
- dynamic multipoles: Fe-shims

Details can be found in [8,9,10]. The required magnet quality of FEL undulators can be achieved with state of the art techniques which can, however, be rather time consuming and are not suitable for a series production.

MAGNET MATERIAL

The new FEL facilities will consist of many undulator segments with totally 10.000s of individual magnets. Today, permanent magnets have typical remanence and angle errors in the order of 1-2% and 1-2°, respectively, where the distributions within one batch can be significantly narrower. The inhomogeneities are important as well and determine the field quality at small gaps. In principle, the required magnet field performance can be achieved with a detailed characterization of the magnets, sorting and shimming. The production process can, however, significantly be simplified if the magnet quality can be improved.

Triggered by the need for high quality magnets for the European X-Ray FEL at DESY and the BESSY Soft X-Ray FEL a BMBF funded joint collaboration between DESY, BESSY and Vacuumschmelze has started. The collaboration has the goal to reduce remanence and angle errors by a factor of 5-10 and to improve the block homogeneity. At a certain level the quality is determined by the geometrical tolerances of the blocks and hence, these tolerances have to be reduced to a level of 10µm. Magnet measurement equipment built at BESSY and DESY has been shipped to the magnet manufacturer

who will use the machines to optimize the production process. BESSY provides a stretched wire system for the characterization of block inhomogeneities whereas DESY has built an automated Helmholtz coil system.

The north south effect (field difference between two opposite sides of a block) is not a useful quantity in particular for APPLE devices where the electron beam is located close to a magnet corner. Block inhomogeneities can be determined by cutting the magnet into slices and measuring the slices in a Helmholtz coil. Results are shown in figure 3 where a systematic variation of the magnetization angle over the position inside the magnet is plotted. The systematic trend can be minimized with an appropriate setting of the production parameters.

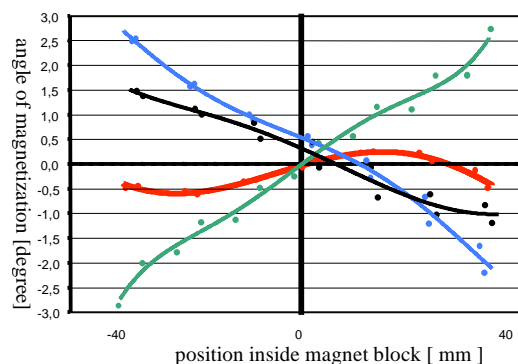


Figure 3: Variation of the magnetization angle inside four individual magnet blocks. The blocks have been produced with different production parameters (by courtesy of Vacuumschmelze, Hanau).

The magnet cutting and the characterization of the slices is time consuming. Similar information can be gathered with the new stretched wire setup in a much shorter time from the complete magnet. The magnet is moved with respect to a single wire in a distance of 5-10mm and induced voltages are measured (figure 4). Measurements from different sides give the information on the magnetization distribution inside the magnet.

Since the measurements are done in a strong field gradient a good positioning accuracy is essential. Temperature stabilized linear motors with absolute encoders and air bearings allow for fast and precise movements. Fe shieldings around the motors reduce the electrical noise.

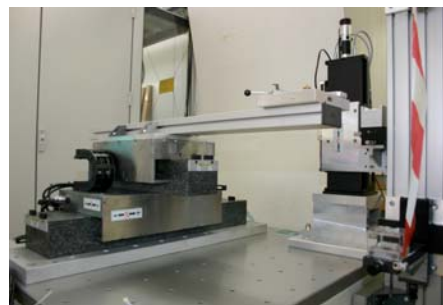


Figure 4: Stretched wire system for the measurement of magnet block inhomogeneities.

Figure 5 shows a reproducibility of 3.0×10^{-4} Tmm for magnets with the magnetization vector parallel to the wire (A-magnets) and 1.5×10^{-3} Tmm for magnets with an orientation perpendicular to the wire (B-magnets). In case of the B-magnets the measurement noise is dominated by a contribution which is proportional to the main signal. A positioning accuracy $< 4.0 \mu\text{m}$ and a temperature stability of $< 0.2^\circ$ is needed to bring the electrical noise to this level.

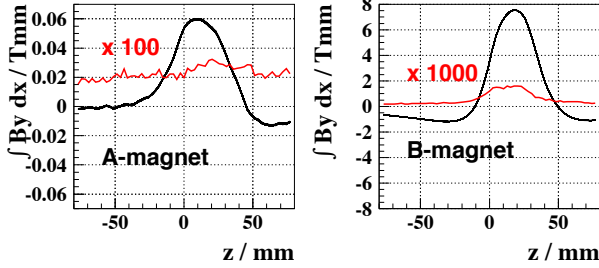


Figure 5: Reproducibilities of the stretched wire system. One hundred blocks of both types have been measured (black) and sigma values (red) have been determined. The distance to the single wire is 10mm and the block dimensions are $40 \times 40 \times 28 \text{ mm}^3$.

TOLERANCES

The tolerances for HGFG and SASE FELs are different from those of storage ring IDs. A good overlap between the photon and electron beam ($\Delta x \leq 0.1 \times (\sigma_{\text{electron}}, \sigma_{\text{photon}})$) defines the maximum trajectory walk off. For a Pierce parameter of 0.001 (BESSY HE-FEL) a maximum variation in the K-parameter of $\pm 5 \times 10^{-4}$ can be tolerated ($\Delta E < 0.16 \times \text{bandwidth}$). This defines the following tolerances: The temperature dependence of the magnet remanence of $0.0011 / ^\circ\text{C}$ requires a temperature stability $\Delta T \leq \pm 0.1^\circ\text{C}$. The gap positioning accuracy must be $\Delta \text{gap} \leq \pm 1 \mu\text{m}$ and the transverse alignment tolerance has to be $\Delta x \leq \pm 40 \mu\text{m}$. The largest contribution to $\Delta K / K$ is attributed to the transverse alignment error (see below). The phase error due to energy spread dominates the total phase error if

$$\Delta \Phi_{\text{rms}} \leq \frac{\sigma_\gamma}{\gamma} \frac{1}{\rho \sqrt{3}}$$

Assuming an energy spread of 2×10^{-4} the tolerance for the phase error of the magnetic field is $\Delta \Phi_{\text{rms}} < 6.6^\circ$ for the BESSY HE-FEL. Apart from quadrupole terms (see later in this paper) static or dynamic multipoles are less important for single pass devices.

The trajectory errors can be measured and minimized with state of the art measurement and shimming techniques. Phase errors below 5° can be achieved even for the complicated APPLE II design without explicit phase shimming as demonstrated for the six BESSY APPLE II devices. A gap positioning accuracy of $\pm 1.5 \mu\text{m}$ has already been achieved [7] (see also next chapter). In the following, we will concentrate on the challenging transverse alignment tolerances.

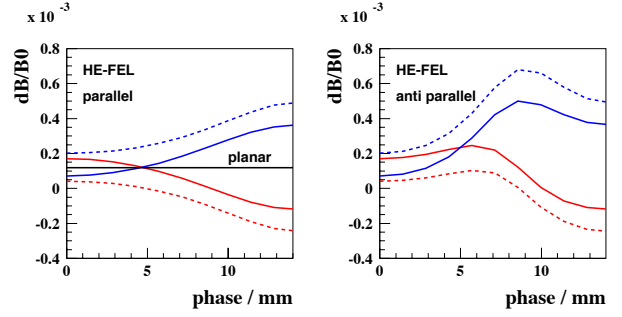


Figure 6: Relative field variation 0.1mm horizontal (red) and vertical (blue) off axis for APPLE III (solid) and APPLE II (dashed) undulator operating in the parallel (left) and antiparallel (right) mode.

The good field region of an APPLE device is significantly reduced as compared to a planar device (figure 6) though it is larger for the APPLE III design as compared to the APPLE II.

In figure 7 the transverse charge distribution of the BESSY FEL electron beam is compared to the field variations in various operation modes. For a maximum transverse displacement of $40 \mu\text{m}$ more than 2σ of the electron beam are within $\Delta K / K < 5 \times 10^{-4}$.

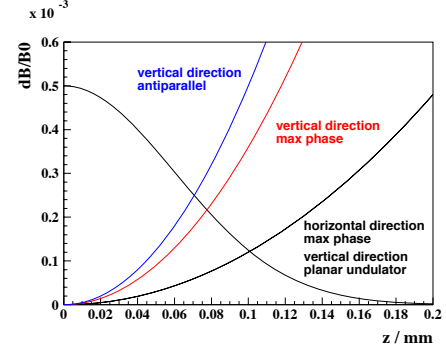


Figure 7: Averaged transverse size of the BESSY FEL electron beam compared to the field roll off for various operation modes.

Figure 8 shows all possible girder misalignments. They are classified as follows:

1. No circle: this movement is uncritical.
2. Black circle: the motion can be minimized with a stiff support structure. The motion is not driven by any force.
3. Blue circle: the movements are well controlled with a closed loop servo system.
4. Red dotted circle: The movement shifts the field amplitude and the center of the good field region. It shows up for antiparallel motion where longitudinal and transverse forces between the upper and lower magnet girders are present.
5. Red circle: The movement enhances $\Delta K / K$. It shows up for antiparallel motion.

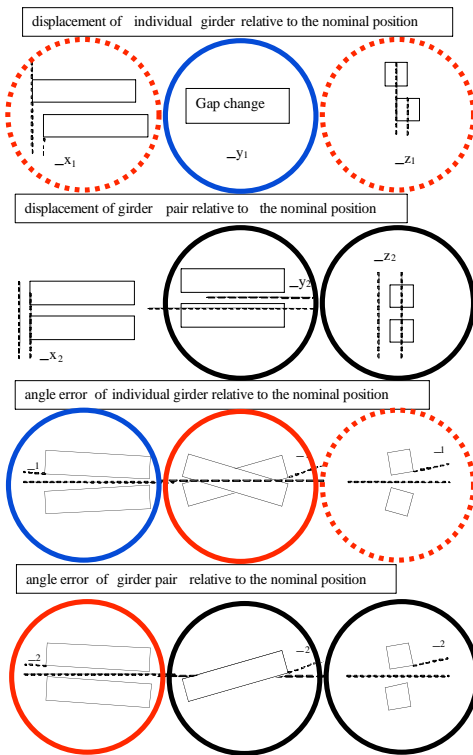


Figure 8: Classification of geometrical tolerances.

SUPPORT AND DRIVE SYSTEM

The tolerances discussed in the previous section define the mechanical design of the support and drive system.

Gap Accuracy

The gap setting has to be done with a closed loop servo system which uses a direct gap reading. The encoders have to be located in a vertical line with the electron beam to avoid Abbe's comparator error [7] (figure 9). Differential thermal expansion coefficients of the support structure (Fe) and the magnet girders and the measurement system (Al) result in a temperature dependent gap error of only $1.1\mu\text{m}/^\circ\text{C}$ for the system described in [7] and can be ignored if compared to the thermal variation of the magnet material remanence.

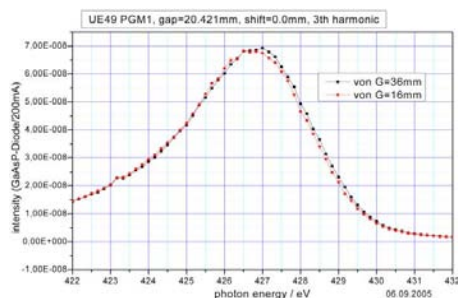


Figure 9: Approaching the third harmonic of the BESSY UE49 from two different directions results in a very small energy shift which corresponds to a gap error of only $\pm 1\mu\text{m}$. The device employs the new measurement system described in [7].

In principle an APPLE II type final amplifier of a HGHC cascade can be realized as a fixed gap device. The energy and polarization tuning can be performed by magnet row movements [11]. The BESSY final amplifiers will be of the APPLE III type. In this case the gap drive is necessary to install and remove the modules from the beam pipe without breaking the vacuum.

The magnets are assembled onto Aluminum girders with a length of up to 4m. They are gimbal-mounted to permit a tapering and to cope with the different thermal expansion coefficient of the Fe-support structure. The straightness of the assembling surfaces of such girders can be within $\pm 8\mu\text{m}$ resulting in a gap variation of only $\pm 15\mu\text{m}$ (figure 10). This remaining gap variation can be reduced to $\pm 6\mu\text{m}$ using appropriate mechanical shims under the magnet holders.

The bending of the magnet girder can be minimized by choosing appropriate locations for the support. The bending can be further reduced by more than one order of magnitude with four supports instead of two using two crossbars inside the magnet girders. This has been demonstrated for the BESSY undulators UE46, UE49 and UE112.

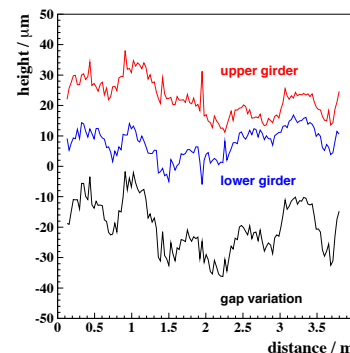


Figure 10: Straightness of upper and lower UE112 magnet girder and corresponding gap variations.

Bearings

In antiparallel mode strong longitudinal and transverse forces between the upper and lower magnet girder show up. The transverse forces can be supported with transverse flexible joints connecting the girders to the support structure. These joints have to permit a longitudinal motion (thermal expansion) and an intentional longitudinal taper of the girders.

The longitudinal forces produce a torque around the vertical axis and around the horizontal (transverse) axis where the strength depends on the location of the joints that keep the girders longitudinally in place. As a result the girders rotate and $\Delta K / K$ on axis is enhanced. The transverse motion can be kept within the acceptable limits with stiff joints between the girders and the support structure. The vertical parallel inclination of the girders can principally be compensated using four motors for the gap drive. Such a drive system can also compensate for the residual transverse girder crossing via a deliberate inclination of the girders. This concept implicates however a complication of the control system

and the gap measurement arrangement. Another solution is the positioning of the longitudinal fixed bearing vertically at the height of the magnets and longitudinally close to the drive system for the row phase. This arrangement eliminates any torque around the transverse axis (figure 11) and hence, any girder inclination or girder bending.

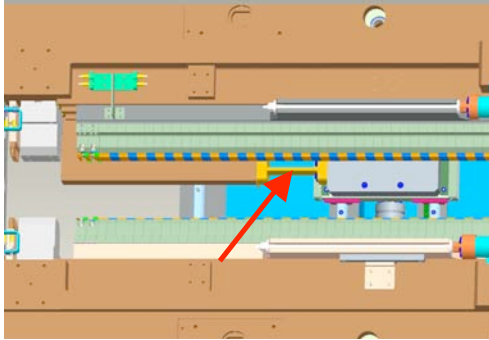


Figure 11: The vertical location of the longitudinal bearing (red arrow) is chosen such that there is no torque around the transverse axis.

Support Structure

The support structure of an APPLE undulator operating in the antiparallel mode has to cope with the strong longitudinal and transverse forces which are absent in a planar or elliptical device.

The support structure can be either a welded structure or a cast structure. The latter one has several advantages:

- The structure can be made extremely stiff without additional effort because literally any shape can be realized.
- A bionic optimization can be applied where material is added at locations with large stress and removed at locations of low stress (figure 12).
- The complete support structure can be cast and milled as a single piece.
- The procedure is suitable for series production since wooden forms can be used for many casts. Modular forms can be adapted to different undulator lengths.

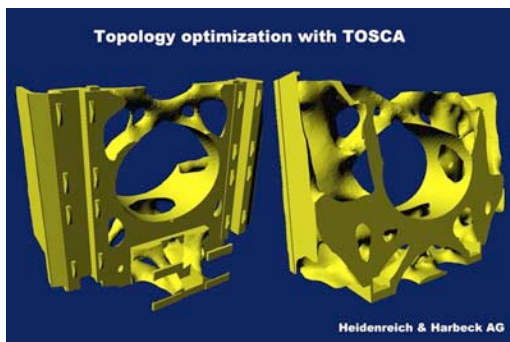


Figure 12: Bionic optimization of the support structure of the BESSY UE112 undulator (by courtesy of Heidenreich und Harbeck AG).

All BESSY undulators are based on cast iron structures. The last APPLE device (UE112) has a single piece support structure (figure 13) which significantly simplifies the assembling procedure.

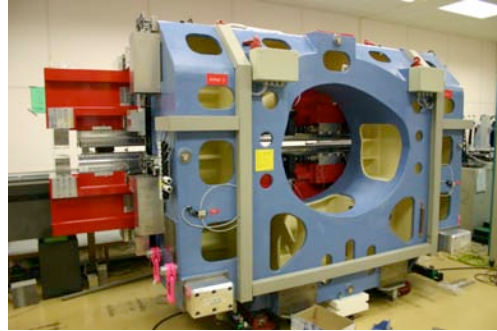


Figure 13: The support structure of the 4m long UE112 is made from a single piece of cast Fe.

Alignment

The magnet centers of all final amplifier modules have to be aligned with an accuracy of $\pm 40\mu\text{m}$ with respect to each other (assuming APPLE type devices). This can not be accomplished with standard alignment tools. Beam based alignment techniques have to be applied instead. For this purpose the modules have to be assembled onto moveable supports with an accuracy of $10\mu\text{m}$.

UNDULATOR FOCUSING

An undulator is a series of alternating dipole magnets which shows an edge focusing. Planar devices focus in the vertical direction. This second order effect can not be described with normal 2-dimensional multipoles. Polarizing devices show also a horizontal defocusing under certain operating conditions which results in an additional focusing in the vertical plane. For Halbach fields the focusing strength in the horizontal plane is given by:

$$K_x = \frac{2 \cdot e^2}{(\gamma mc)^2} k_{x\text{-eff}}^2 \cdot k^2 \cdot \sum_{n=1}^{\infty} (B_{xn}^2 + B_{yn}^2)$$

$$k_{x\text{-eff}}^2 = \sum_{n=1}^{\infty} \frac{B_{xn}^2 \cdot k_{xxn}^2 / n! + B_{yn}^2 \cdot k_{xy n}^2 / n!}{B_{xn}^2 / n! + B_{yn}^2 / n!}$$

and similar for the vertical plane (summation over the Fourier components n). The focusing strength in the antiparallel mode can not be described in this compact form since the fields are not of the Halbach type.

These effects influence the beam size and it has to be considered whether the transverse overlap between the electron beam and the photon beam is still maintained. Figure 14 shows the variation of the horizontal and vertical beam size for the BESSY HE-FEL. The values change by more than a factor of two which is not acceptable. For the BESSY ME- and the LE- FEL the effects are larger by factors of 9 and 45, respectively,

due to the larger period length and larger field (ME- and LE-FEL) and the lower beam energy (LE-FEL). Obviously, additional quadrupoles are essential to keep the beam size within acceptable limits and they have to be adapted during gap drive and row phasing.

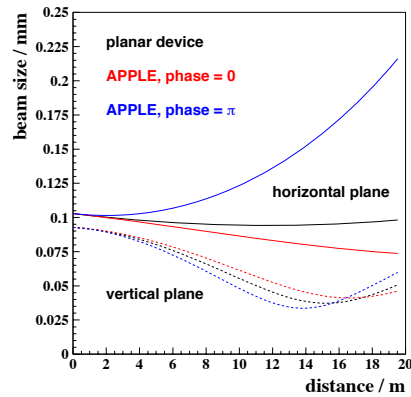


Figure 14: Horizontal (solid) and vertical (dotted) beamsizes within the final amplifier of the BESSY HE-FEL at smallest gap without additional quadrupoles. The data are given for different operation modes of an APPLE III device and for a planar device.

MOTION CONTROL

A cascaded HGFG FEL requires a sophisticated motion control system. Each HGFG stage consists of a modulator and a radiator (maybe several submodules), steerer to compensate residual dipole errors, quadrupoles for tune compensation and phase adapting units between the modules. Between two stages fresh bunch dispersive sections are installed. All components have to be driven in synchronism. Reproducibility is essential and can be realized with closed loop servo systems for motion control, permanent magnet phase adapting units and quadrupoles and air coils to avoid hysteresis effects.

In the following we describe the BESSY system as one possible solution. Other hardware and software concepts are also possible.

Figure 15 shows the control system of a single undulator, the BESSY UE112, which can be adapted to the FEL requirements. The undulator control program runs on a VME-bus based computer called IOC. It is a reliable system and many interface cards are available on the market. The user interface does not run on the IOC but on an independent workstation, which communicates with the IOC via ethernet. In principle, one IOC can control all modules (modulator, radiator, etc.) of one HGFG stage. Four of these systems are required for the BESSY four stages HE-FEL. A fifth IOC operates as a master to synchronize the individual IOCs.

A PLC is useful for a low level safety control of the system checking parameters like air pressure (needed for the brakes), inclination of magnet girders, hard and software limit switches etc.

EPICS is used as a robust and reliable software framework for the undulator control software. All sources are available and it is actively developed in

many research laboratories. Many drivers have been written. Useful tools are available such as an archiver for the process variables or a network protocol for the distribution of the process variables. GUIs can be easily built with a “point and click” tool.

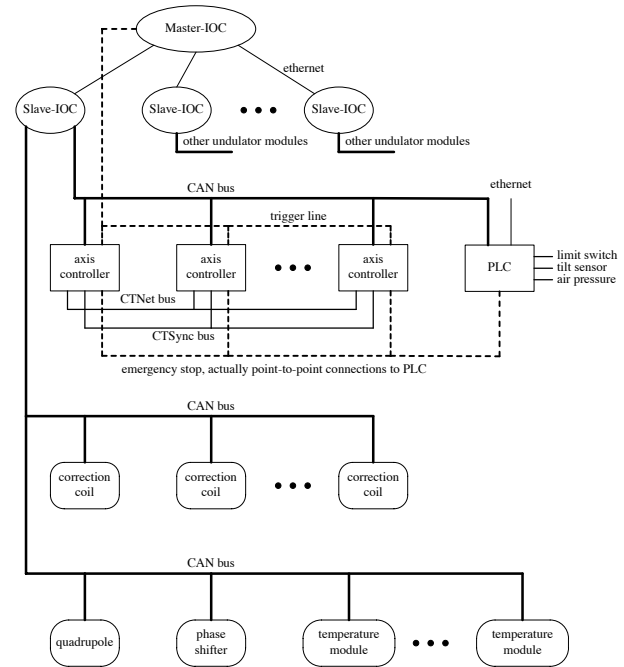


Figure 15: Control system of the BESSY UE112.

Each motor has its own detached motor controller which is connected to the IOC via CAN bus. Absolute linear encoders simplify reference procedures. Modern motor controllers as used for the UE112 can operate several tasks with different priorities. User defined parameters can be stored permanently in the controller and can even be modified during motor movement. The motor controllers can communicate among each other and with the IOC via CTNet (ruggedized version of ARCNet) and a synchronization between the modules can be realized via CTSynch.

BEAM PROTECTION SYSTEM

The electron beam can cause a demagnetization of the undulator magnets if it propagates severely off axis [12-14]. The electrons produce a shower of secondary electrons and photons in the vacuum chamber which may deposit energy into the magnets. Detailed experiments have been done to study the influence of various parameters on the process like the geometry, material, working point of the magnets, temperature etc. [15]. A reduced dose (electron energy > 20 MeV) of 70 kGy produces already a remanence loss of 1% in a typical magnet material with a coercivity of 1800 kA/m [16].

For the layout of a beam protection system the maximum beam charge which may be dumped into the vacuum chamber without loss of performance has to be

determined. In the following we discuss the consequences on the spontaneous radiation spectrum. Simulations for the impact on the stimulated radiation will be done in the future using GENESIS. Two scenarios have been studied where the electron beam hits the vacuum chamber under grazing angles of 1mrad and 0.1mrad, respectively. Due to the small vacuum apertures larger angles are unlikely. Monte Carlo simulations with GEANT [17] have been done for both cases. The deposited charge was 300.000 nC. The magnets have been subdivided into 5x5 (1mrad case) and 7x7 (0.1mrad case) segments (figure 16). Doses have been evaluated for each of the segments.

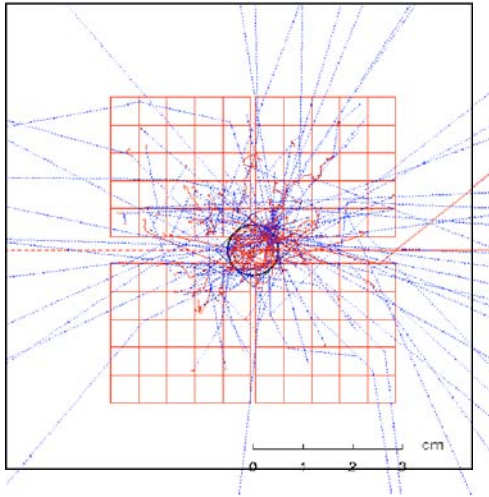


Figure 16: Monte Carlo simulations with GEANT. The geometry for the BESSY HE-FEL with APPLE III magnets (red) and a circular vacuum pipe (blue) has been used. Secondary electrons (red) and photons (blue) are plotted as well.

In the 1mrad case a maximum reduced dose of 700kGy has been detected close to the vacuum pipe. This corresponds to a maximum demagnetization of 10%. Based on the doses in each magnet segment the corresponding remanences have been evaluated. Then, the undulator on axis field has been derived from the contributions of all segments (totally about 70.000 segments). The field reduction close to the point of interaction is 1.6% (figure 17).

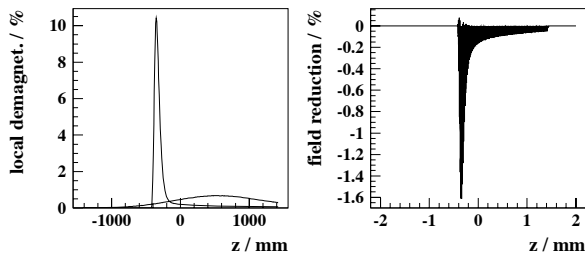


Figure 17: Maximum demagnetization of magnet segments (left) for 1mrad and 0.1mrad angle of incidence and field variation (right) for 1mrad.

In the 0.1mrad case the region of interaction is spread out over more periods and the local degradation is much lower. Since the magnet degradation extends over several periods the trajectory errors are negligible even for the 1mrad case (figure 18). The averaged phase error introduced in this case is 7° (figure 18) which results in a shift of the first harmonic and a splitting of the fifth harmonic (figure 19).

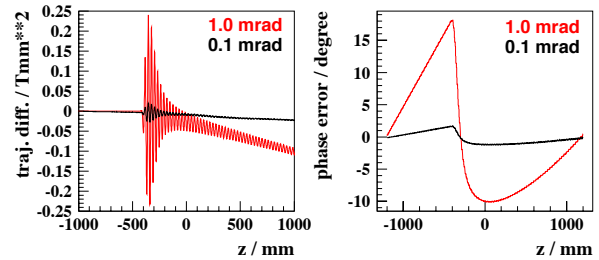


Figure 18: Trajectory errors for angles of incidence of 0.1mrad and 1mrad (left) and phase errors for both cases.

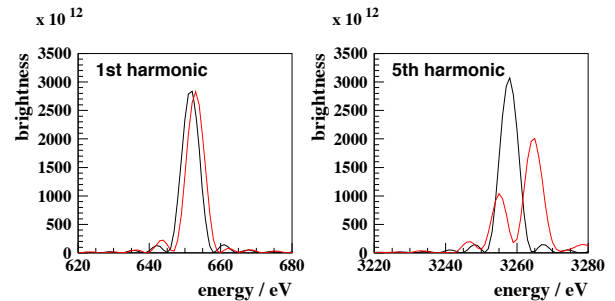


Figure 19: Spectra of the first (left) and fifth (right) harmonic for the unperturbed case (black) and the degraded magnets (red).

Even if the undulator is used only at the first harmonic the spectral shift has to be avoided. The simulations show that a deposited charge of 30.000nC (1mrad) shifts the first harmonic by only $\Delta E/E = 2 \times 10^{-4}$ which is acceptable.

The simulations show that a collimating system for the off axis particles as well as for the off energy particles is essential for a safe operation. The dog-leg collimator for the planned BESSY Soft X-Ray FEL collimates the beam transversally to $\pm 30\sigma$ and energetically to 5%.

Fibre monitors are needed for several purposes: i) A fast interlock system which can switch off the gun laser has to be triggered, ii) information on the total deposited dose is required to estimate the lifetime of the magnets, iii) information on the longitudinal distribution of the deposited radiation helps to detect the hot spots. Two types of fast monitors have been tested at FLASH: i) Cerenkov monitors [18] and ii) fibres for optical time domain reflectometry used in power-meter mode [19]. The latter ones can be used also for spatially resolved measurements. Fibre Bragg gratings can be used as high dose radiation sensors on the scale of many kGy [20].

They provide also information on the spatial distribution of the dose.

CONCLUSION

Various technological aspects for using APPLE undulators in HGHG FELs have been discussed. Experiences gained with APPLE undulators at 3rd generation light sources have been extrapolated and strategies to meet the tight tolerances of HGHG FEL insertion devices have been proposed.

New concepts for the magnet field optimization, for the motion control, for a new support structure and for radiation dose monitoring have already been tested and will be further improved at a 3rd generation facility.

ACKNOWLEDGEMENT

The author thanks M. Scheer for doing the GEANT simulations and H.-J. Bäcker, W. Frentrup, A. Gaupp, S. Gottschlich, G. Pfeiffer, B. Schulz for many fruitful discussions.

REFERENCES

- [1] TESLA-Technical Design Report, TESLA X-FEL, Technical Design Report, 2002-9, 2002.
- [2] Linac Coherent Light Source (LCLS), Conceptual Design Report, SLAC-R-593, 2002.
- [3] T. Shintake, Nucl. Instr. and Meth. in Phys. Res. A, 507 (2003) pp 382-397.
- [4] L. H. Yu, Nucl. Instr. and Meth. in Phys. Res. A, 483 (2002) pp 493-498.
- [5] X. J. Wang et al., Proceedings of the 26th International FEL Conference, Trieste, Italy, 2004, pp 209-211.
C. Bochetta et al., Proceedings of the 27th International FEL Conference, Stanford, CA, 2005, pp 632-685.
The BESSY Soft X-ray Free Electron Laser, Technical Design Report March 2004, eds.: D. Krämer, E. Jaeschke, W. Eberhardt, ISBN 3-9809534-08, BESSY, Berlin (2004).
J. Bahrtdt et al., Proceedings of the EPAC 2006, Edinburgh, Scotland, pp 59-61.
M.-E. Cuprie et al., Proceedings of the 27th International FEL Conference, Stanford, CA, 2005, pp 55-58.
A. Andersson et al., Proceedings of the 26th International FEL Conference, Trieste, Italy, 2004, pp 190-192.
D. Wang et al., Proceedings of 2005 PAC, Knoxville, Tennessee, pp 1961-1963.
J. Wu, Z. Huang, Proceedings of the 27th International FEL Conference, Stanford, CA, 2005, ppxx.
J. Qi-ka et al., Proceedings of the 26th International FEL Conference, Trieste, Italy, 2004, pp 494-497.
- [6] O. Tscherbakoff et al., Proceedings of the EPAC 2006, Edinburgh, Scotland, pp 47-49.
- G. Lambert et al., Proceedings of the EPAC 2006, Edinburgh, Scotland, pp 44-46.
- J. A. Clarke, Proceedings of the EPAC 2006, Edinburgh, Scotland, pp 181-183.
- Gullens et al., Proceedings of the EPAC 2006, Edinburgh, Scotland, pp 142-144.
- [7] J. Bahrtdt et al., Proceedings of the 26th International FEL Conference, Trieste, Italy, 2004, pp 610-613.
- [8] J. Bahrtdt et al., Nucl. Instr. and Meth. in Phys. Res. A, 516 (2004) pp 575-585.
- [9] J. Bahrtdt et al., Proceedings of the International Conference on Synchrotron Radiation Instrumentation, Daegu, Korea, 2006.
- [10] J. Bahrtdt, G. Wüstefeld, Proceedings of the EPAC 2006, Edinburgh, Scotland, pp 3562-3564.
- [11] T. Schmidt et al., Proceedings of the International Conference on Synchrotron Radiation Instrumentation, Daegu, Korea, 2006.
- [12] P. Colomp, T. Oddolaye, P. Elleaume, "Partial Demagnetization of ID6 and Dose Measurements on Certain Ids", Machine Technical Note 1-1996/ID, 1996.
- [13] M. Petra et al., Nucl. Instr. and Meth. in Phys. Res. A, 507 (2003) pp 422-425.
- [14] P. Colomp, T. Oddolaye, P. Elleaume, "Demagnetization of Permanent Magnets to 180 MeV Electron Beam", Technical Report ESRF/MARCH-ID/93-09, European Synchrotron Radiation Facility, ESRF March 1993.
- [15] T. Bizen, T. Tanaka, Y. Asano, D.E. Kim, J.S. Bak, H.S. Lee, H. Kitamaru, Nucl. Instr. and Meth. in Phys. Res. A 467-468 (2001) pp185-189.
M. Marechal, T. Shintake, SRI2003, Conference Proceedings, AIP 705, (2004) pp 282-285.
- [16] H. Schlarb, "Collimation System for the VUV Free-Electron-Laser at the TESLA Test Facility", Thesis Work, Universität Hamburg, DESY-THESIS-2001-055, Nov. 2001.
- [17] GEANT, Detector Description and Simulation Tool, Computing and Networks Division, CERN Geneva Switzerland.
- [18] E. Janata, M. Körfer, H. Schlarb, Nucl. Instr. and Meth. in Phys. Res. A 253 (2004) 256-261.
- [19] H. Henschel, J. Kuhnenn, M. Körfer, F. Wulf, Nucl. Instr. and Meth. in Phys. Res. A, 507 (2003) pp 422-425.
- [20] K. Krebber, H. Henschel, U. Weinhand, „Fibre Bragg Gratings as high dose radiation sensors“, Meas. Sci. Technol. 17 (2006) pp 1-8.